

Viscosity of Liquid ^3He - B near the Superfluid Transition

J. M. Parpia, D. J. Sandiford,^(a) J. E. Berthold,^(b) and J. D. Reppy
Laboratory of Atomic and Solid State Physics and The Materials Science Center,
Cornell University, Ithaca, New York 14853

(Received 15 December 1977)

The normal-fluid viscosity of liquid ^3He - B has been determined in the neighborhood of the superfluid transition using the torsional-oscillator technique of Andronikashvili. In the pressure range from 11.90 to 19.64 bars and for reduced temperatures $t \equiv T/T_c > 0.98$, the B -phase viscosity may be described by $\eta/\eta_c = 1 - [A(1-t)^{1/2} - B(1-t)]$, where η_c is the value of the viscosity at the transition temperature. A and B have the values 6.3 ± 0.2 and 20.0 ± 1.0 , respectively.

In this Letter, we report on measurements of the viscosity and superfluid density in the B phase of superfluid ^3He . These are the first such measurements to possess sufficient resolution to allow a precise examination of the temperature dependence of the normal-fluid viscosity in the immediate vicinity of the superfluid transition. Measurements of the transport properties in the B phase are important, since, from both an experimental and a theoretical point of view, the B phase presents a simpler case for study than the anisotropic A phase. Among the transport properties, the shear viscosity is most easily measured. Following the viscosity measurements of Alvesalo *et al.*,¹ Pethick, Smith, and Bhattacharyya² calculated that the normal-fluid viscosity immediately below the transition in the B phase would decrease in an amount proportional to the energy gap. Subsequently, Ono *et al.*³ predicted that the simple temperature dependence, $(1 - T/T_c)^{1/2}$, characteristic of the energy gap, would dominate only within 3×10^{-4} of T_c . Wölfle⁴ has also calculated the B -phase normal-fluid viscosity.

The early viscosity measurements of Alvesalo *et al.*¹ were made along the melting curve which precluded the possibility of observing the variation of the viscosity near the transition in the B phase. More recently, however, Main *et al.*⁵ and Guernsey *et al.*⁶ have reported viscosity measurements off the melting curve. Neither of these measurements has sufficient resolution to establish the temperature dependence of the normal-fluid viscosity close to the transition. In the work reported here, we have been able to make measurements within 10^{-4} of T_c with a 1% resolution in viscosity.

The data reported here were obtained using the Andronikashvili oscillating-pendulum technique. The design of the oscillating cell was similar to that used by Berthold *et al.*⁷ In the present experiment the refrigeration was provided by a 25-

cm³ cerium magnesium nitrate (CMN) salt pill formed by compression of powdered CMN to 80% of solid density. The thermometry has been very much improved over the earlier experiment⁷ through the use of a separate magnetically shielded CMN thermometer, monitored by a superconducting-quantum-interference-device (SQUID) susceptibility bridge. It was possible to achieve a temperature resolution better than 0.1 μK .

The liquid- ^3He sample under investigation was contained in a disk-shaped region within the bob of the Andronikashvili torsional pendulum. The radius of the ^3He region was 0.42 cm and the height was determined to be 9.5×10^{-3} cm. A hollow beryllium-copper torsion rod connected this fluid to the thermometer and refrigeration cell. The thermometer and the liquid in the viscometer were in close proximity to one another to insure the best possible thermal contact between them.

The temperature scale was established by comparison with a carbon resistance thermometer which had been previously calibrated against the ^3He melting curve down to 30 mK. We use the magnetic temperature T^* obtained from this calibration for the discussion of the results in the normal Fermi-liquid region. However, below the transition temperature T_c , we expect T^* to show strong deviations from T as the CMN approaches its ordering temperature. Therefore, in this region, the CMN susceptibility has been calibrated against T_c as a function of pressure using the "La Jolla" temperature scale.⁸ In terms of our original magnetic temperatures the La Jolla temperature is given by the relation $T = 0.795T^* + 0.299$ mK. We do not quote any results below 2.05 mK, since below this temperature the CMN thermometer is becoming rather insensitive.

The torsional motion of the viscometer cell was driven and detected electrostatically. The oscillator was placed in a feedback loop which varied the drive voltage to maintain a constant

amplitude of motion at the resonant frequency of about 909 Hz. The drive voltage required provided a measure of the damping of the system. At low temperatures the residual damping of the oscillator was small compared with the damping due to the ^3He liquid itself. The amplitude of the oscillation was restricted to about 30 Å on the perimeter of the fluid region. As a result, the maximum relative velocity between the superfluid and the cell wall was on the order of 10^{-3} cm/sec. The frequency was also measured to obtain information on the effective moment of inertia of the fluid entrained through viscous interaction with the walls of the cell during the oscillation. We find that a frequency stability of one part in 10^8 can be achieved by careful control of temperature and fluid pressure. The external ^3He pressure was regulated ± 0.05 bar, which was sufficient to render pressure-induced frequency variations negligible.

Since the ratio, h/R , of the spacing of the viscometer cell to its radius is on the order of 10^{-2} , edge effects have been neglected. The torque exerted on the container during torsional oscillation with angular velocity $\dot{\theta} = \dot{\theta}_0 \exp(-i\omega t)$ is $L = \pi R^4 \dot{\theta} \eta k \tan(\frac{1}{2}hk)$, where $k = (1+i)/\delta$, and $\delta = (2\eta/\omega\rho)^{1/2}$ is the viscous penetration depth. Below the superfluid transition, the density ρ is replaced by the normal fluid density ρ_n . The damping of the oscillator is proportional to the imaginary portion of the torque. The real part is the moment of inertia of the fluid entrained through viscous interaction with the walls. Aside from temperature-independent quantities, the torque depends only on the ratio h/δ of the cell height to the viscous penetration depth.

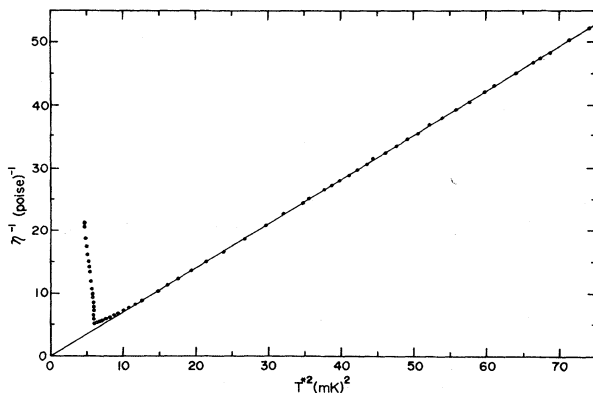


FIG. 1. The inverse of the liquid- ^3He viscosity at a pressure of 15.93 bars as a function of the square of the magnetic temperature.

For temperatures above 100 mK, $\delta \ll h$ and both the real and imaginary parts are small. These quantities grow as the temperature is lowered with the dissipative term reaching a maximum for $h/\delta \approx 2.25$. At lower temperatures in the limit of $\delta \gg h$, the inertial term approaches the solid-body value for the moment of inertia of the fluid, and the damping of the cell becomes proportional to η^{-1} . For sufficiently low temperatures, Fermi-liquid theory predicts that the viscosity of the liquid ^3He will display a T^{-2} temperature dependence. Therefore, in Fig. 1 we show values of inverse viscosity, η^{-1} , obtained at 15.93 bars, plotted against T^* squared. The data above 4 mK are seen to lie on a straight line in agreement with the Fermi-liquid theory. The values of ηT^2 obtained from the straight line are tabulated as a function of pressure in Table I; they agree well with those given by Wheatley⁸ for pressures above 12 bars but are progressively larger with decreasing pressure.

At temperatures below 4 mK the data in Fig. 1 show an interesting departure from the linear Fermi-liquid behavior. At a given temperature this deviation is relatively larger at lower pressures. The pressure dependence assures us that the effect cannot be explained entirely in terms of a distortion of the magnetic temperature scale. We believe that this deviation from Fermi-liquid behavior is related to the increase in quasiparticle mean free path which becomes a significant fraction of the spacing within the Andronikashvili cell at the lowest temperatures.

Below the superfluid transition the viscosity undergoes a rapid decrease; this behavior is reflected in Fig. 1 as a sharp rise in η^{-1} . The tem-

TABLE I. Viscosity and the normal-fluid density parameters.

Pressure (bars)	ηT^{*2} (P mK ²)	A	B	C	D
0	2.55				
4.14	2.13				
9.01	1.75				
11.90	1.63	6.79	22.9	0.54	12.7
14.20	1.49	6.01	18.0	0.56	3.8
15.93	1.43	6.37	20.9	0.57	2.3
17.12	1.38	6.25	20.0	0.52	1.9
19.64	1.27	6.14	18.4	0.56	1.3
23.18	1.18				
25.51	1.14				
29.0	1.07				

perature dependence of the viscosity and normal-fluid density are shown for several pressures in Fig. 2 where the reduced quantities are plotted against temperature. In Fig. 2 we have used lines to represent data where the individual points are too dense to be shown.

A further enlarged view of the viscosity data near the transition for the 17.12-bar run is shown in Fig. 3. The data shown were obtained while both warming and cooling. A gradual decrease of 1.4% in the viscosity occurs over a temperature interval of 5 μ K above the transition. This decrease is seen for all other pressures up to 29 bars for which we have superfluid data and is not related to the rate of warming or cooling. Over this temperature region, an anomalous rise in the period is seen. The period effect is extremely small, being of the order of 2×10^{-4} of the entire period shift in the normal liquid. We are not sure of the origins of these effects. Their causes may be some as yet unsuspected instrumental problems or possibly something more interesting, e.g., a fluctuation precursor such as suggested by Emery.⁹

The viscosity data below the transition have been fitted by the expression $\eta/\eta_c = 1 - [A(1-t)^{1/2} - B(1-t)]$ over the temperature interval $1 \geq t \geq 0.99$. The values of A and B obtained for sev-

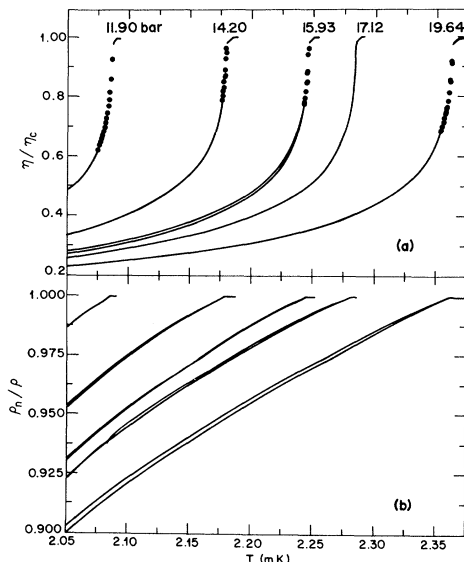


FIG. 2. (a) The reduced viscosity and (b) the normal-fluid density as functions of temperature. The La Jolla temperature scale has been used for these plots. The different pressures, in bars, at which these data were obtained are indicated above the viscosity curves. At all pressures except 11.90 bars the data from several different runs are shown.

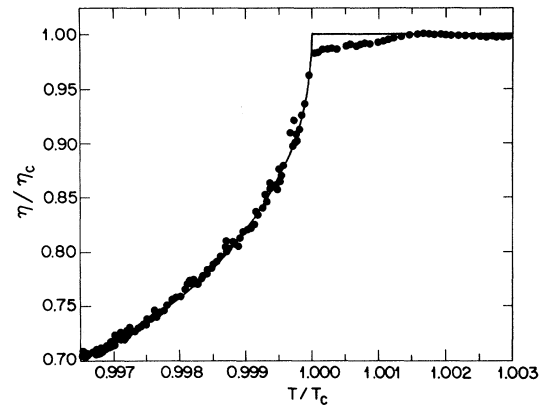


FIG. 3. An enlarged view of the viscosity as a function of temperature. The data were obtained at a pressure of 17.12 bars. The curve drawn through the data below the superfluid transitions is the fitted function, $\eta/\eta_c = 1 - [6.25(1 - T/T_c)^{1/2} - 20.0(1 - T/T_c)]$.

eral different pressures measured in the B phase are listed in Table I. No evident pressure dependence is seen.

In Fig. 4 we plot the change in reduced viscosity, $\delta\eta/\eta_c = (\eta_c - \eta)/\eta_c$, vs $1 - T/T_c$ for the 17.12-bar run. Except for a limited region where $1 - T/T_c$ is less than approximately 5×10^{-4} , the change in viscosity cannot be adequately represented by an expression linear in the energy gap. This result is in accord with the estimate of Ono *et al.*³

The transition temperature T_c is chosen as the temperature where the reduced viscosity commences to drop sharply. T_c can be determined within a 0.1- μ K temperature interval, which is

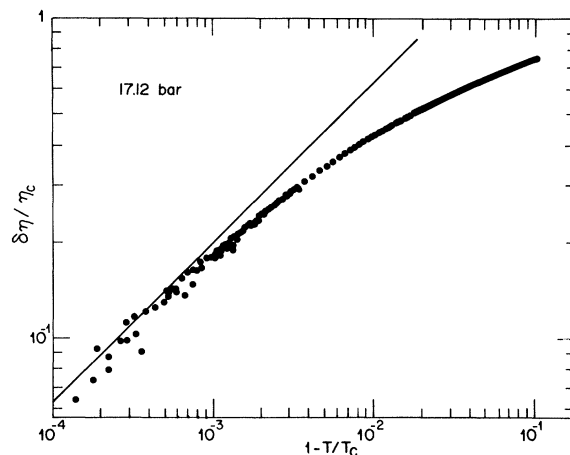


FIG. 4. The change in viscosity below the transitions, normalized by the value at the transition, plotted on a log-log scale as a function of the reduced temperature difference, $1 - T/T_c$. The straight line indicates a $(1 - T/T_c)^{1/2}$ temperature dependence.

smaller than the scatter in Fig. 4. The drive voltage is monitored continuously and is observed to give a signature at T_c whose sharpness is consistent with the Q of the viscometer, ensuring that the temperature is homogenous to within the precision of the measurement.

The B -phase normal-fluid density data, shown in Fig. 2(b), have been fitted by a function of the form $\rho_n/\rho = 1 - C(1-t) - D(1-t)^2$, for $t > 0.9$. The coefficients C and D are listed in Table I. No significant pressure dependence is seen in the coefficient of the linear term.

The authors would like to acknowledge the assistance of Professor R. A. Buhrman with the SQUID thermometry, and the help of Dr. E. N. Smith with the construction of the Andronikashvili cell.

This work has been supported by the National Science Foundation through Grants No. DMR 75-08624 and No. DMR 76-21669 and by the National Science Foundation through the Cornell Materials Science Center Grant No. DMR 76-01281, MSC Report No. 2951.

^(a)Present address: Physics Department, Schuster Laboratory, The University of Manchester, Manchester M13 9PL, England.

^(b)Present address: Bell Laboratories, Murray Hill, N. J. 07974.

¹T. A. Alvesalo, H. K. Collan, M. T. Lopenen, and M. C. Veuro, *Phys. Rev. Lett.* **32**, 981 (1974); T. A. Alvesalo, H. K. Collan, M. T. Lopenen, O. V. Lounasmaa, and M. C. Veuro, *J. Low Temp. Phys.* **19**, 1 (1975).

²C. J. Pethick, H. Smith, and P. Bhattacharyya, *Phys. Rev. Lett.* **34**, 643 (1975); P. Bhattacharyya, C. J. Pethick, and H. Smith, *Phys. Rev. B* **15**, 3367 (1977).

³Y. A. Ono, J. Hara, K. Nagai, and K. Kawamura, *J. Low Temp. Phys.* **27**, 513 (1977).

⁴P. Wölfle, to be published.

⁵P. C. Main, C. W. Kiewiet, W. T. Band, J. R. Hook, D. J. Sandiford, and H. E. Hall, *J. Phys. C* **9**, L397 (1976).

⁶R. W. Guernsey, J. R. McCoy, M. Steinback, and J. K. Lyden, *Phys. Lett.* **58A**, 26 (1976).

⁷J. E. Berthold, R. W. Giannetta, E. N. Smith, and J. D. Reppy, *Phys. Rev. Lett.* **37**, 1138 (1976).

⁸J. C. Wheatley, *Rev. Mod. Phys.* **47**, 415 (1975).

⁹V. J. Emery, *J. Low Temp. Phys.* **22**, 467 (1976).

Role of Intrinsic Plasmons in Conduction-Band X-Ray Photoemission from Solids

David R. Penn

National Bureau of Standards, Washington, D. C. 20234

(Received 14 November 1977; revised manuscript received 7 December 1977)

I show that intrinsic plasmons are created in x-ray photoemission experiments on the conduction bands of simple metals. Unlike the core case, the plasmons are produced by many-body effects and are a direct consequence of electron correlation. A theory of the intrinsic plasmon production is given and a calculation of the electron energy-loss spectra in conduction-band x-ray photoemission from Mg and Na is presented. The calculation takes into account both intrinsic and extrinsic plasmon production and the agreement with experiment is good.

In recent years x-ray photoemission spectroscopy (XPS) from the conduction bands of metals has become an important tool in the determination of electronic densities of states. The purpose of this Letter is to show that intrinsic plasmons are created in XPS experiments on the conduction bands of simple metals and that they play an important role in the XPS loss spectra, i.e., in the plasmon satellites. A theory of intrinsic plasmon creation is presented which shows that the physics of the process is new and quite different from the case of intrinsic plasmon production in core-level XPS. The XPS loss spectra provide the most direct experimental evidence for intrinsic plasmon production and calculations for Mg

and Na are reported and compared to experiment. The contributions of intrinsic plasmons to the first loss peak are estimated to be $\approx 37\%$ and 44% in Mg and Na, respectively.

In the case of XPS from the core levels of nearly-free-electron metals a typical loss spectrum consists of several peaks centered at E_0 , $E_0 - \hbar\omega_p$, $E_0 - 2\hbar\omega_p$, etc., where $\hbar\omega_p$ is the plasma energy. The peaks represent electrons that have excited zero, one, two, etc., plasmons prior to escaping from the solid. Almost ten years ago Lundqvist¹ suggested that a large fraction of the loss spectra was due to intrinsic plasmon production, a process in which the core electron is photoexcited and simultaneously one or more plasmons are